DERIVATION OF PARTICULATE DIRECTIONAL INFORMATION FROM ANALYSIS OF ELLIPTICAL IMPACT CRATERS ON LDEF

P.J. Newman, N. Mackay, S.P. Deshpande, S.F. Green and J.A.M. McDonnell
Unit for Space Sciences
Physics Laboratory
University of Kent
Canterbury
Kent CT2 7NR, U.K.
Phone: [44] (227) 459616 Fax: [44] (227) 762616

SUMMARY

The Long Duration Exposure Facility provided a gravity gradient stabilised platform which allowed limited directional information to be derived from particle impact experiments. The morphology of impact craters on semi-infinite materials contains information which may be used to determine the direction of impact much more accurately. We demonstrate the applicability of this technique and present preliminary results of measurements from LDEF and modelling of interplanetary dust and space debris.

1 INTRODUCTION

The Long Duration Exposure Facility (LDEF) was retrieved in January 1990 after 69 months exposure to the Low Earth Orbit (LEO) space environment. In addition to the many experiments specifically designed to detect impacting dust particles of natural and terrestrial origin, any external surface of the spacecraft was exposed to potential damage from which particle properties may be determined.

LDEF was a gravity gradient stabilised, 12-sided cylinder with its long axis pointed approximately towards the Earth. One face (denoted East, Ram, or 9) was constantly pointed towards the spacecraft's orbital velocity vector (figure 1 illustrates the geometry). Definition of the exact orientation, deduced after recovery, incorporates tilt (rotation about the North-South axis - perpendicular to the Space-Earth axis) and an offset angle (rotation about the Space-Earth axis such that the true orbital velocity vector was offset to the North pointing direction). The distribution of impact data around the different faces of LDEF gives some information on the directionality of impacting particles. However resolution is limited since each face is accessible to impacts from a hemisphere and the normals to each peripheral face are only 30° apart. By deducing actual impact directions for individual impact sites from the shape of the crater, it is possible to determine the orbital direction causing such an impact. A number of well characterised solid surfaces are available for such a study, including the aluminium clamps supporting each experiment tray. Some of these clamps were available for examination at high magnification, yielding crater morphologies for further study (section 2). This paper describes how these data may be derived and compared with models of interplanetary and space debris particle orbit distributions.

2 IMPACT CRATER MORPHOLOGY

Several LDEF clamps have been examined using the Unit's Philips 525M scanning electron microscope to identify possible impact craters. Images of each of these sites were then taken from normal to the clamp surface and at ± 7.5° to the normal. The two off-axis images were examined using a stereo viewer, enabling positive identification of true hypervelocity impacts sites. The stereo

reconstructions of these impacts allowed the depth and the maximum and minimum diameter of each crater to be measured, using the plane of the clamp as a reference point. For "elliptical" craters, an estimate of the direction of impact could also be made using criteria obtained from experimental impact studies at oblique angles. Such impacts form elliptical craters with high raised lips on the side from which the impact occurred (the entrance side) and flattened lips on the exit side. The crater walls are steeper and sometimes undercut on the entrance side. The shape of the crater is not truly elliptical, but egg-shaped, being deeper and wider at the entrance side (Kinecke, 1960; Bryan, 1960) (see figures 2 and 3). "Ellipticity" used here is determined from the semi-major and semi-minor axes, a and b

$$e = (1 - b^2/a^2)^{1/2} \quad (1)$$

Craters on LDEF surfaces have been placed in three categories:

"Circular" - Irregularities in the surface and uncertainties in the exact crater edge result in ellipticities smaller than 0.3 being indistinguishable from circular.

"Elliptical" - Craters with morphology characteristic of oblique impacts. The direction of impact can be estimated with an accuracy of approximately 20 degrees.

"Undefined" - Craters with elliptical shapes but unusual morphology. It is not possible to determine which was the entrance or exit side or even if the crater was the result or an oblique impact.

Several examples of craters from LDEF clamps are illustrated in figure 2.

The relationship between eccentricity of an impact crater to the angle of impact has not yet been determined. Impact experiments into metals (eg Kinecke, 1960) indicate that craters are circular for impact angles up to a critical angle, above which they exhibit the properties described above (Bryan, 1960). As the particle velocity is increased, the critical angle increases (Culp, 1959). For material with no cohesive strength, the critical angle is large (>60° from the normal) and dependent on velocity and physical properties of the target and projectile (Gault and Wedekind, 1978). Impacts in solid non-metallic targets (Mandeville and Vedder, 1971) show central craters and spallation regions but the characteristic crater morphology for oblique impacts was easily distinguishable from craters produced by irregular particles. These experimental results apply to a range of materials and velocity and impact angle regimes but the relationship between crater ellipticity and such properties is not well quantified. It is theoretically possible to constrain this function using the relationship between the observed ellipticities of craters and the ratios of fluxes observed on different faces of LDEF (section 5). Much of the experimental data have been obtained in relatively low velocity regimes which favour non-circular crater production, whereas typical velocities in space are considerable larger. One might therefore expect most impact craters to be circular (as is the case for the Moon). However, a significant number of craters on LDEF are non-circular and therefore contain information on the direction of impact.

3 MODELLING OF MICROMETEOROID AND SPACE DEBRIS IMPACT DIRECTIONS ON LDEF

3.1 Impacts on LDEF

The impact model is based on input geocentric particulate velocity and flux or spatial density distributions, and a definition of the LDEF orbit and orientation. The resultant impact velocity on each face of LDEF is calculated for each geocentric particle velocity and direction. The results are then presented as $F(v,\eta,\psi)$ where v = impact speed in km s^{-1} and η,ψ are impact direction as defined in figure 1. v is specified in 1 km s^{-1} bins and η and ψ in 10° bins.

Parameters used in the model are

LDEF mean altitude = 460 km

LDEF orbital velocity = 7.64 km s^{-1}

Offset = 8°
Tilt = 1.1°
Earth radius = 6378 km
Effective atmospheric height = 150 km.

3.2 Interplanetary dust model

Interplanetary dust particles are assumed to have an isotropic geocentric flux distribution. The velocity distribution is assumed to be the same as found for photographic meteors (Erickson, 1968) corrected for the difference in escape velocity at LDEF's altitude (compared with typical meteor altitudes). Earth shielding removes particles from directions originating in a cone of semi-angle 73° from the Earth direction. If absolute numbers of impacts as a function of particle mass are required then the mass distribution for flux of interplanetary dust at a heliocentric distance of 1 A.U. (Grün et al, 1985) multiplied by a gravitational enhancement factor, $G = 1 + 0.76\ (r_e/r)$, is used.

3.3 Space debris model

The geocentric space debris velocities in a number of altitude and latitude cells are determined from the known orbital distribution of tracked debris to give a three dimensional model. The distributions of altitude, eccentricity and inclination are included, but the longitudes of nodes and lines of apsides are assumed to be random. Further details of the debris model are given by Green & McDonnell, ["A numerical model for characterisation of the orbital debris environment." Proc. of Workshop on "Hypervelocity Impacts in Space", Canterbury, Kent, UK, July 1991, in press].

4 INTERPRETATION OF RESULTS

4.1 Crater ellipticity

Elliptical craters measured on clamps can be presented in polar plots with angle = η and radial distance = e. The ellipticity, e, is a function of ψ (and other factors). Only a small number of clamps have so far been inspected to a resolution of 20μm with complete sampling. Craters as small as 4μm have been detected but sampling at this size is incomplete due to SEM resolution and clamp surface roughness. Table 1 provides a summary of LDEF surfaces for which analysis may be performed. Table 2 contains the data for the clamps measured so far, which are presented in figure 6 and discussed in section 4.4.

4.2 Interplanetary Dust

The Interplanetary dust model produces, for each face, $F_i(v,\eta,\psi)$, the flux in v, η, ψ bins, calculated assuming an isotropic interplanetary flux of 1 particle m^{-2} sr^{-1}. Results from the model are represented by polar plots with angle = η and radial distance = R_i where

$$R_i = K_i \sum_{v} \sum_{\psi} F_i(v,\eta,\psi) \sin\psi \qquad (2)$$

and K_i is a scaling constant (which can be used to incorporate the absolute flux of particles as a function of particle mass). The model plots therefore give an indication of the sum of the ellipticity of craters in a given direction. When the relationship between ψ and e is determined, a more direct comparison may be made.

Figure 4 shows the results for the East, West, North, South, Space and Earth faces for the interplanetary dust model. The same K_i value has been used for each face to illustrate the relative "fluxes" of elliptical craters on each face (see caption for relative plot scale).

On the East face the effect of the Earth shielding cone is immediately apparent. The angle corresponding to Earth shielding for a stationary spacecraft at this altitude is approximately 73° above the Earth direction. However, for a moving spacecraft the effective Earth shielding cone is rotated forward in the direction of motion (i.e. true East here). As a result, the 105° and 255° bins are much more significantly affected by Earth shielding than would be expected for a static spacecraft. The 8° offset causes the North side (and therefore the leading edge) to have a higher R_i value in general than the South side.

On the West face the R_i values are roughly a factor of 10 lower due to the spacecraft's velocity (requiring objects to "catch up" with the spacecraft). The effect of the spacecraft's motion on the Earth shielding region is again apparent, producing a decreased effective shielding angle so that the 105° and 255° bins are not affected. As before the 8° offset causes an increase in the values of R_i on the North side.

The North and South faces show the affect of the spacecraft's velocity as an enhancement of R_i in the East direction.

The Space face is the only one which is unaffected by Earth shielding. The maximum R_i value occurs offset by 8° from the East (Ram) direction.

Most of the impacts on the Earth face are blocked out by Earth shielding resulting in Ri values some 15-20 times lower than Space. The ratio of East-to-West Ri values is much less than for the Space face due to the spacecraft's tilt. The 1.1° tilt leans the Space face towards East and so increases the values on the East side and decreases those on the West. Conversely, the Earth face is tilted towards the West so producing a relative enhancement of the values on the West.

4.3 Space debris

The space debris model produces, for each face, $F_d(v,\eta,\psi)$, the flux in v, η, ψ bins, expressed as a fraction of the total debris population (with the constraints of the assumptions described in section 3.3). Results from the model are represented by polar plots with angle = η and radial distance = R_d where

$$R_d = K_d \sum_{v} \sum_{\psi} F_d(v,\eta,\psi) \sin\psi \qquad (3)$$

and K_d is a scaling constant (which can be used to incorporate the absolute flux of debris particles as a function of particle mass or size). Figure 5 illustrates the results for the entire debris population which can impact the East, West, North, South, Space and Earth faces in the same form as the interplanetary component. The same value of K_d has been adopted for each face (see caption for plot scales) but does not indicate the absolute numbers of debris particles.

The East face distribution indicates a high flux of elliptical craters (large R_d) from the North and South directions. This would be expected from the large proportion of debris in circular orbits (e=0) which would only intersect LDEF in a plane perpendicular to the LDEF orbit radius vector and

therefore along the North-South line. The values are not exactly on the North-South line as a result of the 1.1° tilt of the space face to the ram direction (causing a shift towards the space face direction) combined with the 10° quantisation of the data. The value of R in the South direction is greater than that of the North. This seems to contradict the known 8° offset towards the North face implying that the North face flux will be higher than that for the South. However, the R_d value is the impacting flux weighted by the sine of the impact angle to give a function representative of crater ellipticity (shallow impact angles producing higher ellipticity). Because of the "butterfly" distribution associated with space debris impact angles the 8° offset reduces the mean incidence angle γ for the North lobe compared with the South and the sine ψ weighting therefore produces a higher R_d value in the South direction.

The West face experiences 500 times less elliptical impact craters than the East. The nominal West face should not receive impacts from debris in circular orbits, although debris in eccentric orbits can impact the West face if their mean altitudes are higher than that of LDEF. Due to the encounter geometry we would therefore expect impact directions to be symmetrical about the North-South line (impact before or after perigee) and the Earth-Space Line (impact from direction of higher or lower latitudes than LDEF). The 8° offset allows a tiny fraction of circular orbit particles to impact the West face from North and South directions at near grazing incidence with the 1.1° tilt shifting these directions slightly towards the Earth direction. The model angular distribution is highly sensitive to the small number of elliptical orbits with access to the West face.

The South and North faces have approximately the same number of elliptical craters as East, all originating from the East direction. The impact distribution on the South (North) face has a maximum R_d close to the East/West line with the 1.1° tilt causing a small shift towards the Space face.

The space face distribution shows the butterfly distribution associated with space debris towards the East face direction, albeit a factor of 100 less than the East face distribution. The 1.1° tilt is seen in the east bias of the distribution with a small number of impacts in the west direction from particles in highly eccentric orbits.

The Earth face distribution, at 1000 times less than the East face, is somewhat distorted by the quantisation effects of the model. The 1.1° tilt can be seen from the impacts in the West direction as this now becomes accessible to debris impacts with the addition of the 8° offset.

4.4 Impact Analysis

Figure 6 illustrates the data obtained so far for elliptical craters on clamps. The East face has very few impacts from the Earth direction due to Earth shielding. The results imply a mixture of the two sources with a distribution of impact directions from North through Space to South with rather more from the North/Space quadrant (natural) but with an excess lying on the North/South line (space debris).

On the North face the impacts have occurred predominantly from the East/Space quadrant with the impacts tending towards the East. This agrees with a combination of the natural and debris models which predict impacts from debris only from the East direction and for the natural particles predominantly from the forward facing direction. The single impact in the Space/West quadrant is probably a natural particle, as the model predicts a very low probability of debris impacts from that direction.

All of the impacts that have been measured on the South face come from the East/Space quadrant, again with a bias towards the ram direction. The two impacts which came directly from the East could be either space debris or natural particles, whereas the two other impacts 30 degrees from the ram direction should be of natural origin.

Impacts on the Space face would be expected predominantly from within 90° of the ram direction. However, of the two measured impacts one is from the West direction.

These preliminary results illustrate the potential power of the technique and the need for scanning of larger areas to improve the statistics, and for chemical analysis of as many sites as possible to determine their source independently.

5 CALIBRATION OF THE ELLIPTICITY FUNCTION

Currently, the crater morphology is only being used to determine impact angle (η). However, the precise angle from the normal (ψ) at which this occurs is unknown and the way in which the various aspects of the crater morphology (eccentricity, entrance and exit lip heights and crater wall slopes) vary with respect to the impact angle, velocity, material density and strength are not well defined. A series of non-normal impact experiments using the Unit's Van de Graaff particle accelerator and light gas gun have recently been initiated to investigate these relationships.

With a calibrated fit between the impact angle and crater morphology the impact ellipticities that have been measured may be converted to real particle directions. Since the mean impact velocity will vary with direction for any face this must be accompanied by use of dynamical models. The total fluxes on each face of LDEF provide a means of testing the validity of such a relationship, since the angular distribution predicted from the elliptical crater dimensions must be consistent with the relative numbers impacting each face. In theory it should be possible to derive this relationship from the flux data itself, but a combination of low angular resolution and the apparent nature of the relationship at small impact angles (shape almost independent of ψ for values less than ~55° has been derived for consistency of LDEF fluxes) mean that it is not well constrained.

6 CONCLUSIONS

The space debris and interplanetary particle models predict radically different impact angular distributions for each face of LDEF. The measured properties of elliptical craters provide a potentially powerful tool for determination of the relative contributions, at different particle sizes, of these two sources, which is complementary to chemical analysis. Further laboratory experiments on non-normal impacts are required to produce quantitative empirical relationships between crater morphology and impact direction, velocity, etc., which will allow the true three-dimensional distribution of debris velocities to be determined.

Acknowledgements

We acknowledge the financial support of the UK Science and Engineering Research Council, and F. Hörz for constructive criticism of the original manuscript.

References

Erickson, J. E.: (1968). "Velocity distribution of sporadic photographic meteors." J. Geophys. Res., **73** 3721-3726.

Bryan, G.M.: (1960). "A Model of Oblique Impact." Hypervelocity Impact, 4th Symposium, Air Proving Ground Center, Eglin Air Force Base, Florida, APGC-TR-60-39 (III), section 33.

Culp, F.L.: (1959). "Volume-Energy Relation for Craters Formed by High-Velocity Projectiles." Hypervelocity Impact, 3rd Symposium, Armour Research Foundation of Illinois Inst. of Technology, Chicago.

Gault, D.E. and Wedekind, J.A.: (1978). "Experimental Studies of Oblique Impact." Proc. 9th Lunar Planet Sci. Conf., 3843-3875.

Grün, E., Zook, H. A., Fechtig, H. and Giese, R.H.: (1985). "Collisional balance of the meteoritic complex", Icarus **62** 244-272.
Humes, D.H.: (1984). "Space Debris Impact Experiment", LDEF Mission 1 Experiments, (Eds. Clark, L.G., Kinard, W.H,., Carter, D.J. and Jones, J.L.) NASA SP-473 136-137.
Kineke, J.H. Jr.: (1960) "An Experimental Study of Crater Formation in Metallic Targets." Hypervelocity Impact, 4th Symposium, Air Proving Ground Center, Eglin Air Force Base Florida, APGC-TR-60-39 (I), section 4.
Mandeville, J.-C. and Vedder, J.F.: (1971). "Microcraters Formed in Glass by Low Density Projectiles." Earth and Planet. Sci. Lett. 11, 297-306.

Bibliography

See, T., Allbrooks, M., Atkinson, D., Simon, C. and Zolensky, M.: (1990). "Meteoroid and debris impact features documented on the Long Duration Exposure Facility, a preliminary report", Publication #84, JSC # 24608, 583 pp.

Table 1. Surfaces on LDEF available for crater ellipticity determination.

Surface	Material	Faces	Surface area	Crater size	Comments
Frames, Clamps, Flanges	Aluminium	All	~24m^2	a>2μm	Limit due to surface roughness. Restricted angular coverage
IDE experiment	Aluminium	Not E	~25m^2	a>0.1μm	(Humes 1984)
MAP Foils	Aluminium, Brass	E, W, N, S, Sp	~0.6m^2	0.1μm<a< (1.5-30μm)	Non-perforation required

Table 2. Ellipticity data for clamps measured to date.

Face	area, m^2	Clamps measured circular (e<0.3)	elliptical	undefined (see text)	Total clamp area available
East	5.7x10^{-3}	12	17	9	0.07 m^2
(a<20μm)	4.4x10^{-4}	23	6	6	
West	5.7x10^{-3}	0	0	0	0.07 m^2
North	5.7x10^{-3}	10	5	3	0.07 m^2
South	5.7x10^{-3}	14	4	0	0.07 m^2
Space	1.14x10^{-2}	14	2	0	0.49 m^2
Earth	-	-	-	-	0.42 m^2

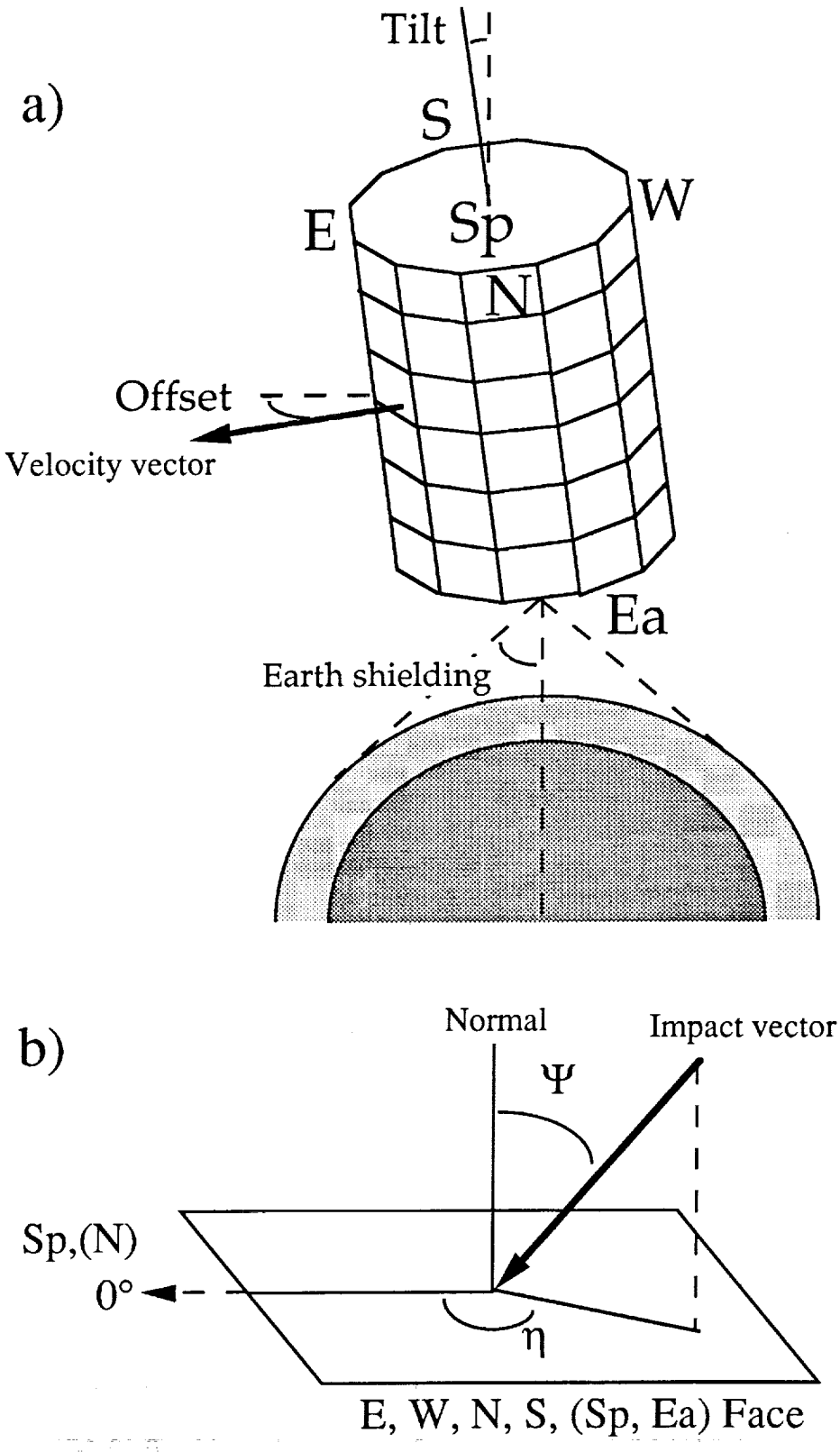

Figure 1. a) Orientation of LDEF in space showing tilt and offset angles.
b) Definition of impact angles on an individual face of LDEF.

a)

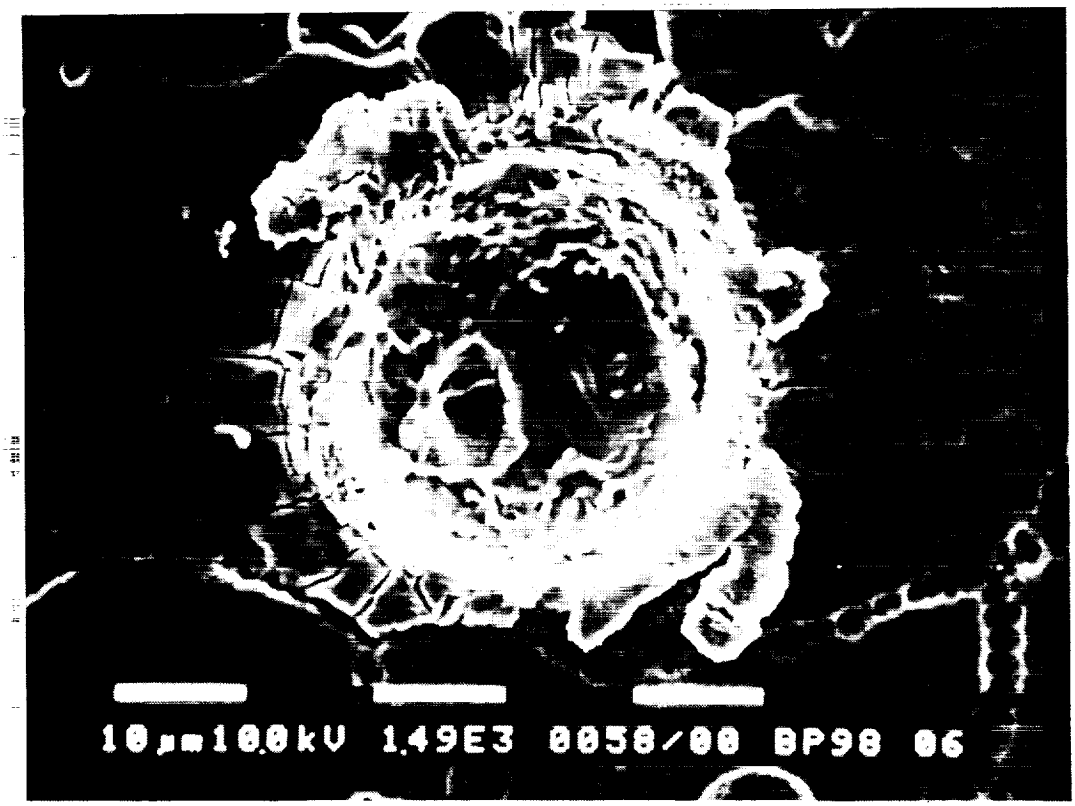

b)

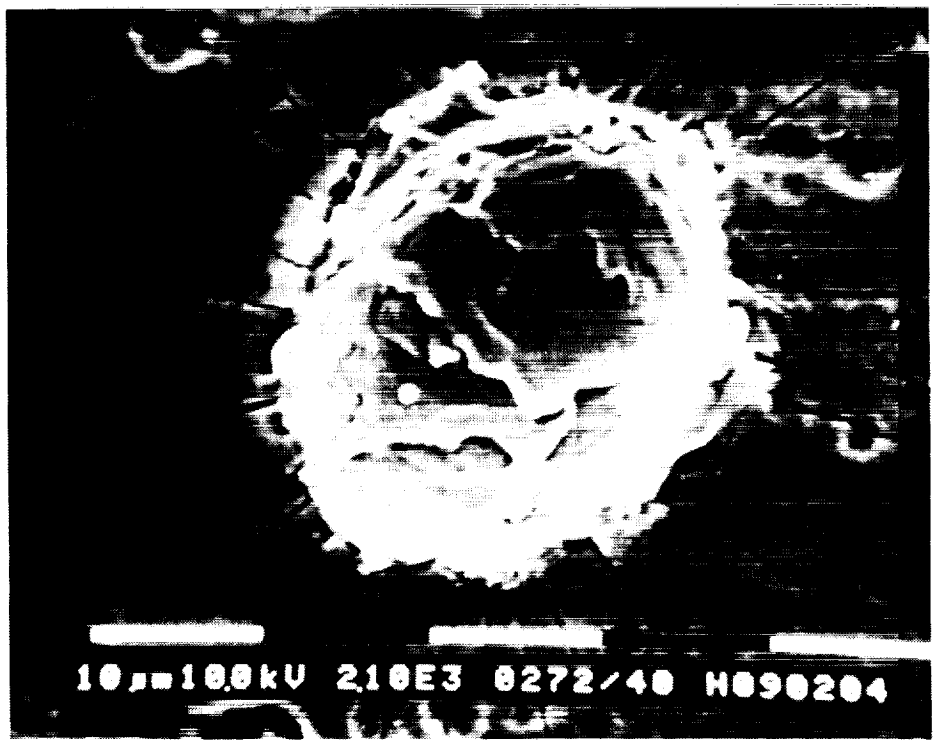

Figure 2. Photomicrographs of typical impact craters on LDEF clamps.
a) circular: a = 34.8±0.9 µm, b = 34.8±0.9 µm, e < 0.3,
b) elliptical: a = 30.5±0.8 µm, b = 22.6±0.7 µm, e = 0.67±0.05,
c) undefined: a = 105±3 µm, b = 68±2 µm, nominal e = 0.77±0.03,

2c

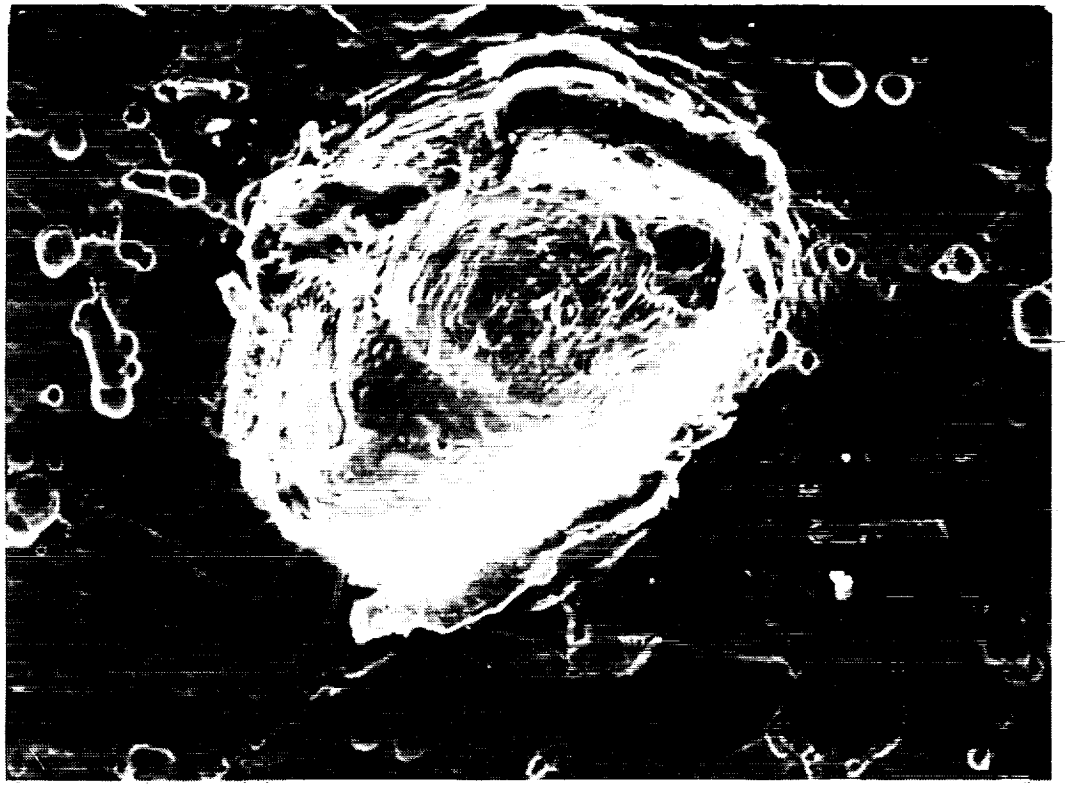

Figure 2. Concluded.

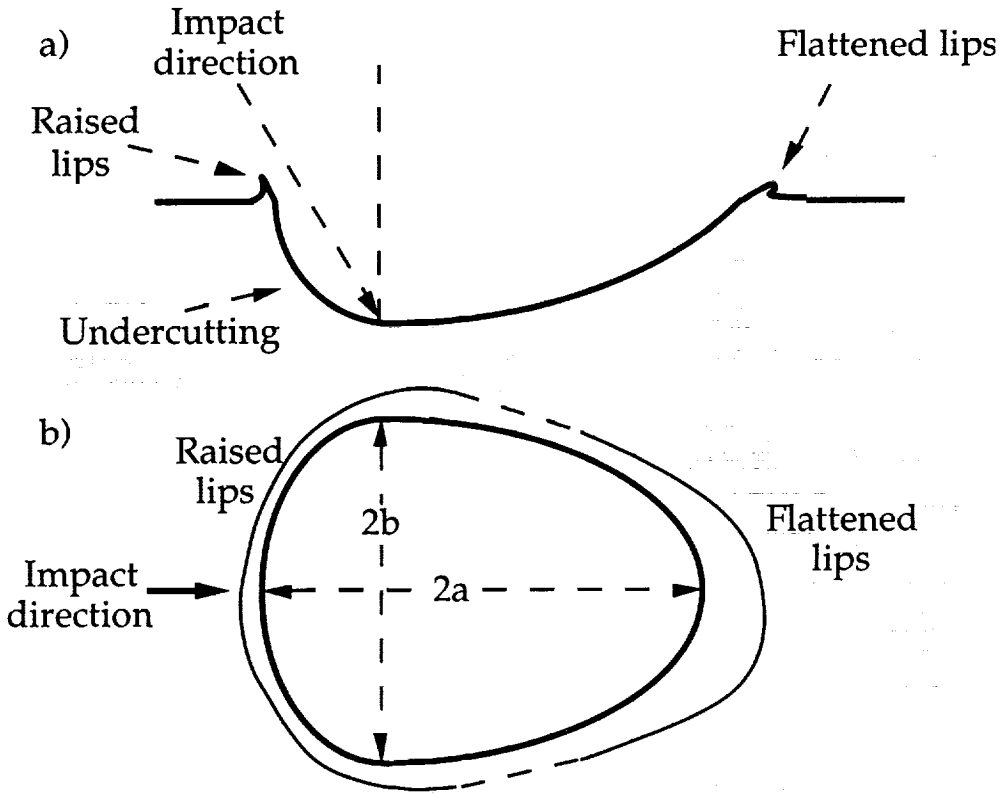

Figure 3. Schematic of crater shapes, a) profile, b) plan.

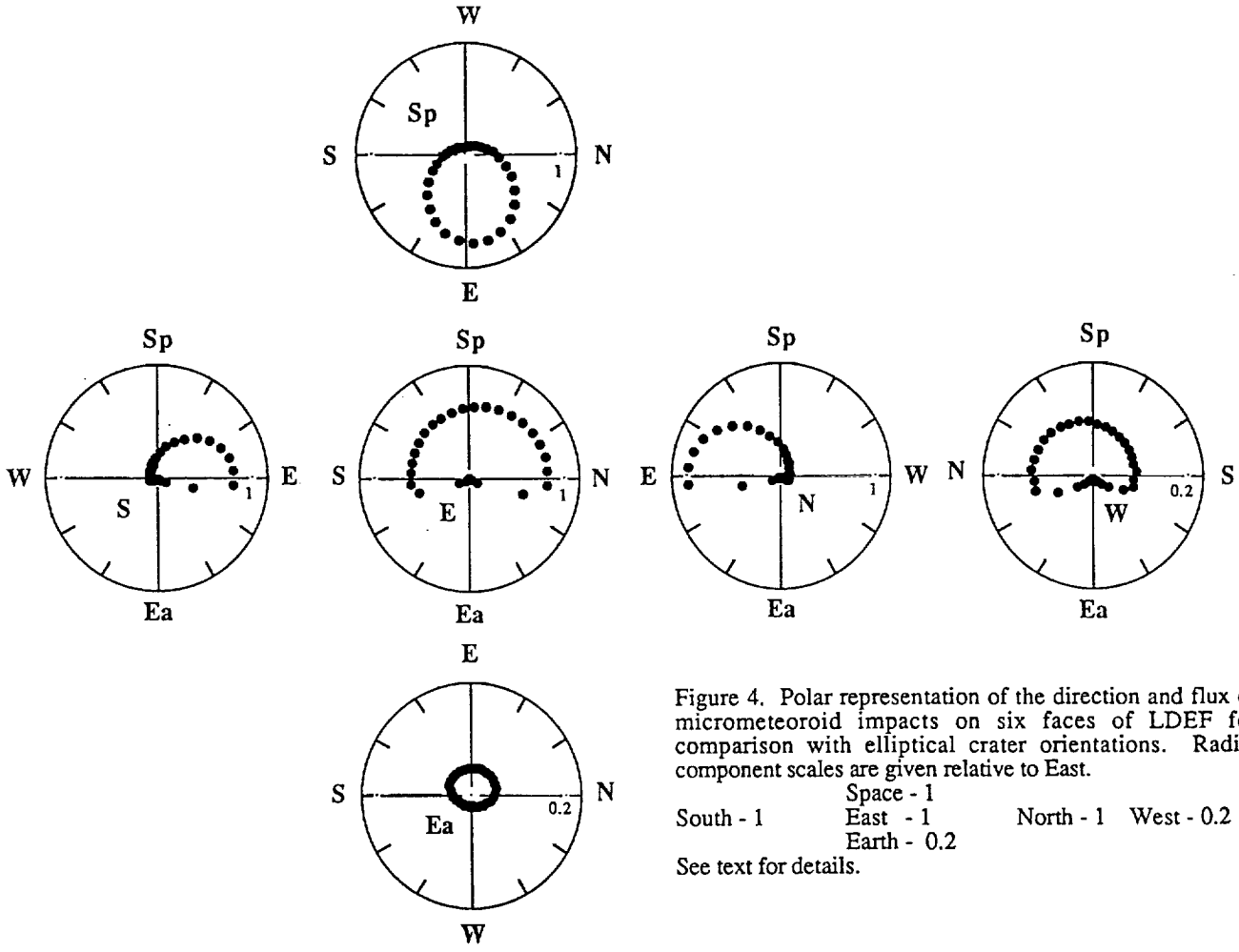

Figure 4. Polar representation of the direction and flux of micrometeoroid impacts on six faces of LDEF for comparison with elliptical crater orientations. Radial component scales are given relative to East.

Space - 1
South - 1 East - 1 North - 1 West - 0.2
Earth - 0.2

See text for details.

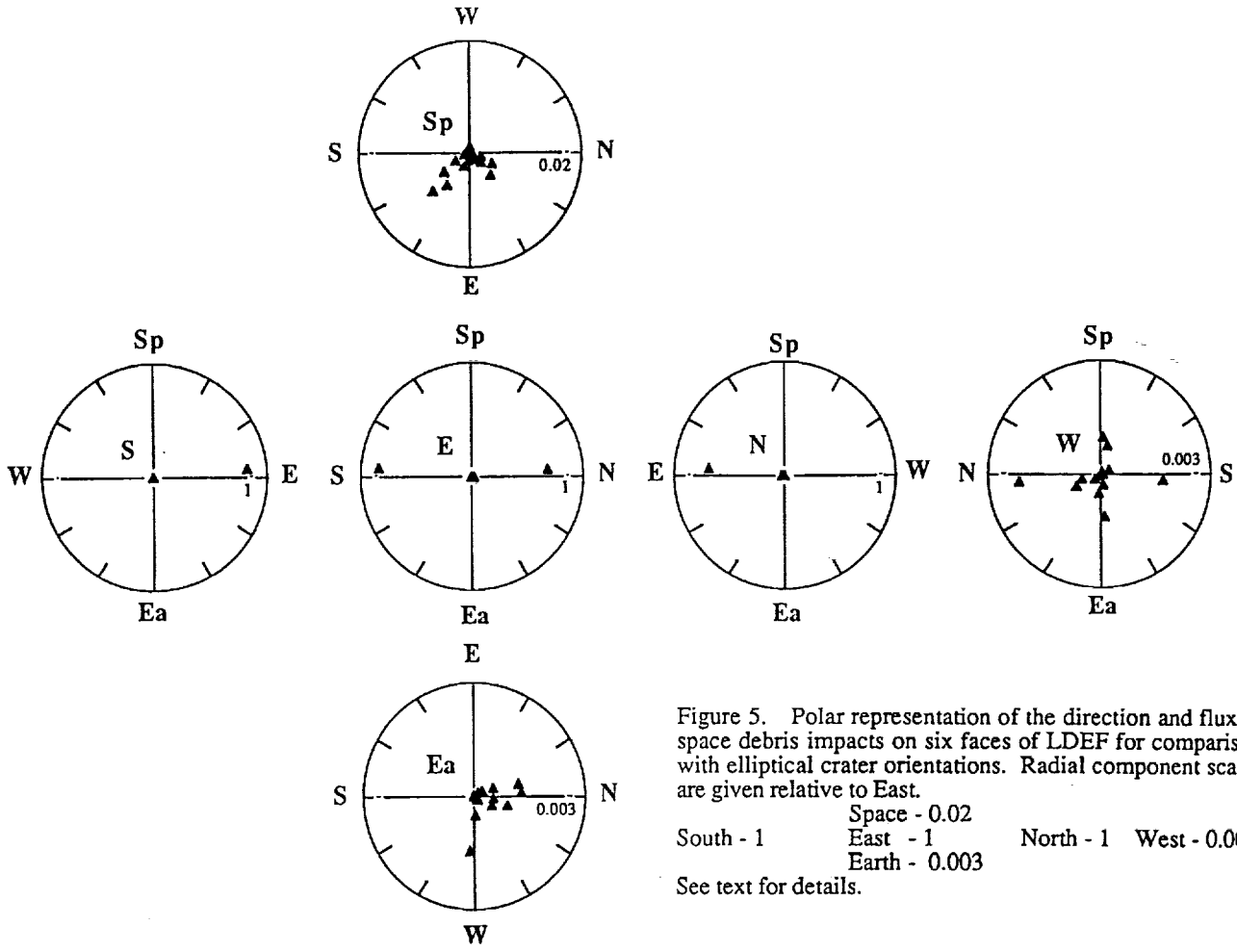

Figure 5. Polar representation of the direction and flux of space debris impacts on six faces of LDEF for comparison with elliptical crater orientations. Radial component scales are given relative to East.

Space - 0.02
South - 1 East - 1 North - 1 West - 0.003
Earth - 0.003

See text for details.

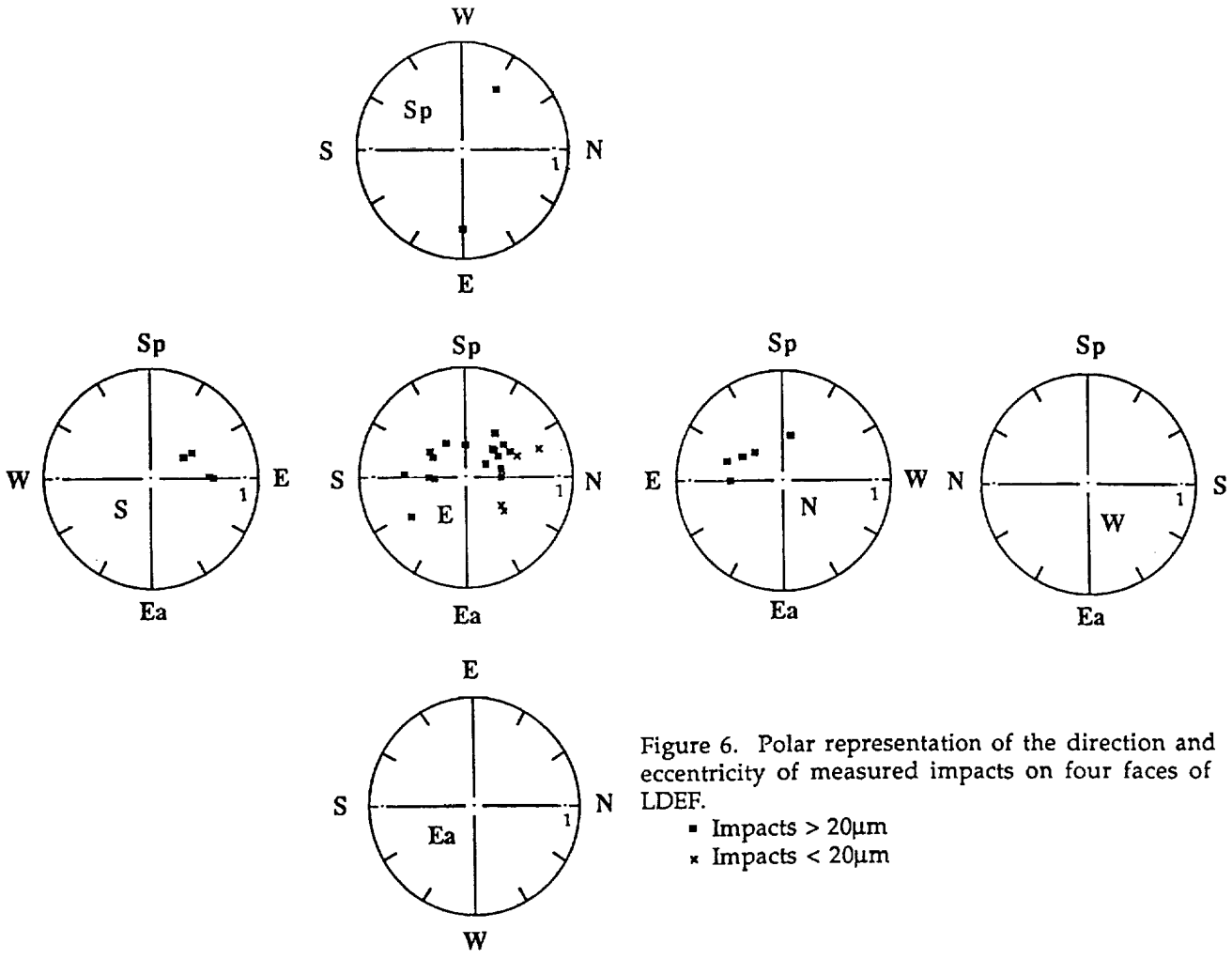

Figure 6. Polar representation of the direction and eccentricity of measured impacts on four faces of LDEF.

- ▪ Impacts > 20μm
- × Impacts < 20μm